Asian Journal of Applied Sciences



Asian Journal of Applied Sciences 7 (7): 607-620, 2014 ISSN 1996-3343 / DOI: 10.3923/ajaps.2014.607.620 © 2014 Knowledgia Review, Malaysia

Synthesis and Characterization of Zn_{1-x}Cd_xS Thin Films Prepared by the Spray Pyrolysis Technique

¹M. Kamruzzaman, ²Kamal Uddin Azad and ³Jiban Podder

¹Department of Physics and Materials Science, Center of Super-Diamond and Advanced Films (COSDAF), City University of Hong Kong, Hong Kong Special Administrative Region, People's of Republic China

Corresponding Author: Kamal Uddin Azad, Government Sherpur Mohila College, Sherpur, Bangladesh

ABSTRACT

The $\operatorname{Zn_{1-x}Cd_xS}$ ($0\le \times \le 1$) thin films have been prepared using a low cost and simple spray pyrolysis technique onto preheated glass substrates at temperature 523 K. The surface morphology, structural, optical and electrical properties of the as-deposited and annealed $\operatorname{Zn_{0.20}Cd_{0.80}S}$ films were studied by optical microscopy, Energy Dispersive X-ray (EDX), X-Ray Diffraction (XRD), UV-visible spectroscopy and Vander Pauw method, respectively. The films are shown inhomogeneous surfaces, less defined grain boundaries. The elemental analysis (EDX) revealed that the deposited films are of Zn, Cd and S compositions. X-ray diffraction patterns indicated that the as-deposited films are amorphous in nature and the annealed film is found to be crystalline structure. The average grain size of the annealed film is found to be 8-47 nm and its value increases with the increase of annealing temperature. Various optical constants viz., optical band gap, extinction coefficient, refractive index and dielectric constant have been studied. The direct optical band gap energy of the as-deposited and annealed films is varied from 3.64-2.40 eV and 2.62-2.1 eV, respectively. The dc electrical conductivity increases with the increase of temperature and also with Cd doping.

Key words: II-VI semiconductors, thin films, spray pyrolysis, band gap, conductivity

INTRODUCTION

The II-VI and III-V groups' compound semiconductors are of great importance due to their applications in various fields of science and technology. Zinc Sulphide (ZnS) is the II-VI group semiconductor with a direct band gap of 3.50-3.70 eV (Berger and Pamplin, 1993). It is used as a key material for light emitting diodes, electroluminescent displays, cathodoluminescent displays, multilayer dielectric filters, blue light emitting laser diodes and antireflection coating for heterojunction solar cells (Nicolau et al., 1990; Marquardt et al., 1994; Kumar et al., 2008; Haase et al., 1991; Hirabayashi and Kozawaguchi, 1986). ZnS is widely used as a window layer in hetrojunction photovoltaic solar cells because the wide band gap decreases the window absorption loses and improves the short circuit current of the cell (Shaban et al., 2011). On the other hand, cadmium sulfide (CdS) is also the II-VI group compound semiconductor with a band gap of 2.42 eV (Archbold et al., 2005). It is a low resistivity semiconductor and can be used as a high transparent conducting sulphide in the visible range and high light trapping agent. CdS has been doped with a wide variety of elements (ZnS, Cu₂S, Al, Co, In, Sn, Se, Te, etc.) to meet the demands of several

²Government Sherpur Mohila College, Sherpur, Bangladesh

³Department of Physics, Bangladesh University of Engineering and Technology (BUET), Dhaka, 1000, Bangladesh

application fields such as thin film solar cells (Ristova and Ristov, 1998), electrochemical cells (Jadhav et al., 2001), gas sensor (Kanemitsu et al., 2002) and it is also employed in high efficiency solar cells formed with Cu₂S/ZnCdS and Cu₂S/CdS (Hall and Meakin, 1979; Saraf, 2012; Nakada et al., 1994). Among the binary compounds PbS, SnO₂, In₂O₃, CdO and WO₃, the ZnS and CdS are the most typical inorganic semiconductor materials because they play important roles in both basic science and application fields. Various technological applications mentioned above need new and alternative materials with developed properties. The properties of Zn_{1.x}Cd_xS thin films are lie in between the properties of ZnS and CdS. Doping of Cd with ZnS can be tuned the band gap i.e., $\mathrm{Zn_{1x}Cd_xS}$ changes the band structure as a result, it makes the material much more attractive for the fabrication of solar cells (Reddy and Reddy, 1992; Oladeji et al., 2000). The Zn_{1-x}Cd_xS thin films have been widely used as a wide band gap window material in heterojunction photovoltaic solar cells (Reddy and Reddy, 1992; Oladeji et al., 2000) and in photoconductive devices (Torres and Gordillo, 1992). Incorporation of Cd into Zn_{1.x}Cd_xS modified the optical window of the heterojunction and also the diffusion potential (Chynoweth and Bube, 1980; Kulkarni et al., 2001) and it can lead to an increase in photocurrent by providing a match in the electron affinities of the two materials. This ternary Zn_{1.x}Cd S compound is also potentially useful as a window material for the fabrication of p-n junctions without lattice mismatch in devices based on quaternary materials like CuIn_xGa_{1-x}Se₂ or CuIn(S_xSe_{1-x})2 (Yamaguchi et al., 1992). With respect to this aim, we tried to improve some physical characteristics of Zn_{1-x}Cd_xS thin films prepared by spray pyrolysis.

Several techniques have been used to produce ZnS thin film such as chemical method (Borah and Sarma, 2008), electron beam evaporation (Lytvyn et al., 2001), chemical bath deposition (Jayanthi et al., 2007; Ubale et al., 2007a), sol-gel method (Bhattacharjee et al., 2002), metal organic chemical vapor deposition (Seo et al., 2005), radio frequency magnetron co-sputtering (Glass et al., 2007) and Spray Pyrolysis Deposition (SPD) (Glass et al., 2007; El Hichou et al., 2004; Islam and Podder, 2009). All the referred methods have complex setup and are expensive but Spray Pyrolysis Deposition (SPD) has some advantages over those techniques such as very simple, low cost experimental set up from an economical point of view and it could be employed for the large scale deposition production of undoped and doped thin films without applying any high vacuum system (Bedir et al., 2002). Although, much study has been done on the electronic and optical properties of the binary ZnS, CdS and partially doped $\rm Zn_{1.x}Cd_xS$ (upto x = 0.5) thin films (Chynoweth and Bube, 1980; Oztas and Bedir, 2001; Ilican et al., 2007) but there is no information available on the structural, optical and electrical properties of the ternary Zn_{1x}Cd_xS (0 ≤×≤1) thin films prepared by spray pyrolysis technique. In this point of view, the ternary Zn_{1.x}Cd_xS thin films have been deposited on the glass substrate using SPD system at a relatively low temperature 523 K so as to reduce the preparation cost and studied their structural, optical and electrical properties, respectively.

MATERIAL AND METHODS

Preparation of this films: The $Zn_{1-x}Cd_xS$ (x = 0.00, 0.20, 0.40, 0.60, 0.80 and 1.00) thin films were prepared using the spray pyrolysis method (SPD) from aqueous solution of zinc acetate $Zn(CH_3COO)_2.2H_2O$ (0.1 M), thiourea (NH₂CSNH₂), (0.2 M) and cadmium acetate $Cd(CH_3COO)_2.3H_2O$, (0.1 M). Experimental set up and the films preparation is in the previous published study (Kamruzzaman *et al.*, 2012). The possible reaction may take place at the surface of the heated substrate as follows:

$$Zn_{l-x}(CH_3COO)_3 \cdot 2H_2O + Cd_x(CH_3COO)_2 \cdot 3H_2O + NH_2CSNH_2 \\ \frac{523K}{Decompose} \rightarrow Zn_{l-x}Cd_xS + NH_3 \\ \uparrow + CO_2 \\ \uparrow + steam \\ \uparrow + CO_2 \\ \uparrow + steam \\ \uparrow + CO_3 \\ \uparrow + steam \\ \uparrow$$

Characterization: The thicknesses of the films was measured using the setup of Fizeau fringes method. Surface morphology of the films was characterized using the swift photomicroscope and elemental analysis by Energy Dispersive X-ray (EDX) (Inspect IS50 FEI Company). The transmittance and absorbance data were collected at room temperature using double beam UV-Vis spectrophotometer (UV-1601PC Shimadzu, Japan) in BCSIR, for wavelength 300-1100 nm. The X-Ray Diffraction (XRD) data of as-deposited and annealed films were taken by PHILIPS model "X'Pert PRO XRD System with $\text{CuK}_{\alpha}(\lambda = 1.54178 \text{ Å})$, radiation diffractometer. Vander Pauw method was used to investigate the electrical property of the films in the temperature range 303-403 K.

RESULTS AND DISCUSSION

Surface morphology: The surface morphology under 1200 magnification of the as-deposited $Zn_{1,x}Cd_xS$ thin films are shown in Fig. 1a-f. From optical surface property in Fig. 1, it is noticed that film surface becomes homogeneous increasingly coarse and less define grain boundaries with the increment of Cd, which can be described as a conglomerate random roughness to be the characteristic of an amorphous nature.

Some cracks are observed on the ZnS film (Fig. 1a) and Cd precipitation is also observed on the CdS film (Fig. 1f). But, some opaque portions of clusters are introduced on the films due to Cd incorporation. However, surface become homogeneous and smooth for x = 0.80 (Fig. 1e). So it may be necessary to limit the degree of Cd present in these films for applications like solar cells, particularly when spray pyrolysis is used as the fabrication technique. Figure 1g-i shows the surface optical photographs of the annealed $Zn_{0.2}Cd_{0.8}S$ film. From these figures, we see that annealing temperature greatly affect on the films morphology. With the increase of annealing temperature surface homogeneity, quality, crystallinity increases as a consequence of Cd diffusion over the surface well and reduces defects and surface roughness.

Figure 2 shows the EDX spectra of $Zn_{1-x}Cd_xS$ films (for x=0.00, 0.80 and 1.00) and the corresponding at percentage is given in Table 1. From Table 1 we see that sulphur deficiency occurred in all samples, because sulphur has great affinity towards oxygen, so it might have converted to SO_2 and then evaporated. In Fig. 2a and c two peaks arise in the spectra corresponding to Zn and S and Cd and S which confirmed ZnS and CdS films, respectively. However, for x=0.80 the elemental Zn, Cd and S peaks arise in the spectra satisfied that the prepared $Zn_{1-x}Cd_xS$ ($0 \le x \le 1$) films are composed of Zn, Cd and S.

Table 1: Atomic percentage of different compositions of $\mathrm{Zn_{1-x}Cd_xS}$ thin films

Compositions	Atomic (%)		
	Zn	Cd	S
ZnS	53.22	00	46.78
$\mathrm{Zn}_{0.8}\mathrm{Cd}_{0.2}\mathrm{S}$	43.28	11.46	45.26
$\begin{split} &Zn_{0.8}Cd_{0.2}S\\ &Zn_{0.6}Cd_{0.4}S\\ &Zn_{0.4}Cd_{0.6}S\\ &Zn_{0.2}Cd_{0.8}S \end{split}$	32.55	23.29	44.16
$\mathrm{Zn}_{0.4}\mathrm{Cd}_{0.6}\mathrm{S}$	23.10	34.66	42.24
${ m Zn}_{.0.2}{ m Cd}_{0.8}{ m S}$	11.58	40.15	48.27
CdS	00	52.24	47.76

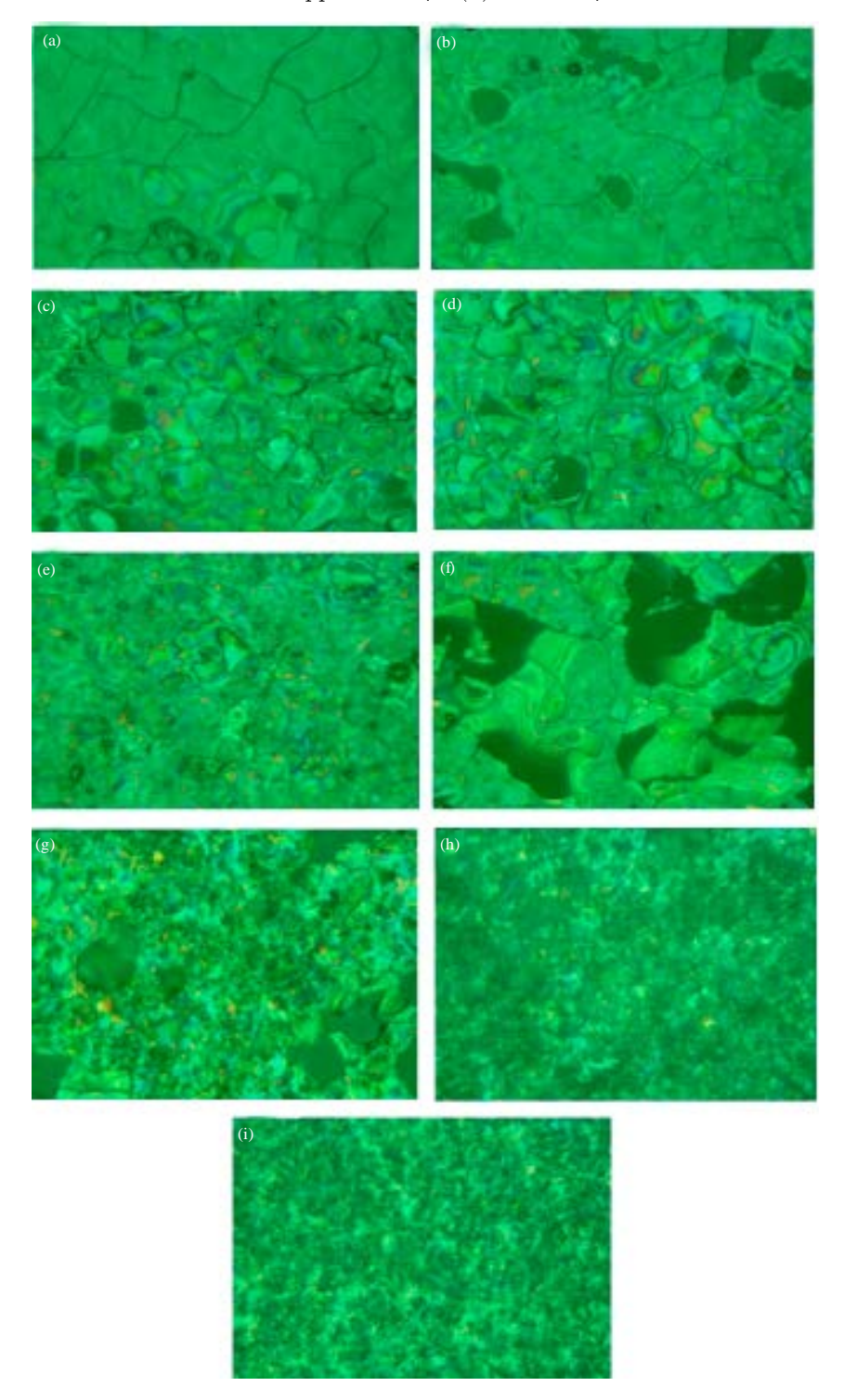


Fig. 1(a-i): Experimental set up of spray pyrolysis method, (a-f) Surface optical photograph of as-deposited $\rm Zn_{1-x}Cd_xS$ films for x = 0, 0.20, 0.40, 0.60, 0.80 and 1.00 under 1200 magnification and (g-i) Surface optical photograph of the annealed film at temp. 673 K, 773 K and 873 K under 1200 magnification

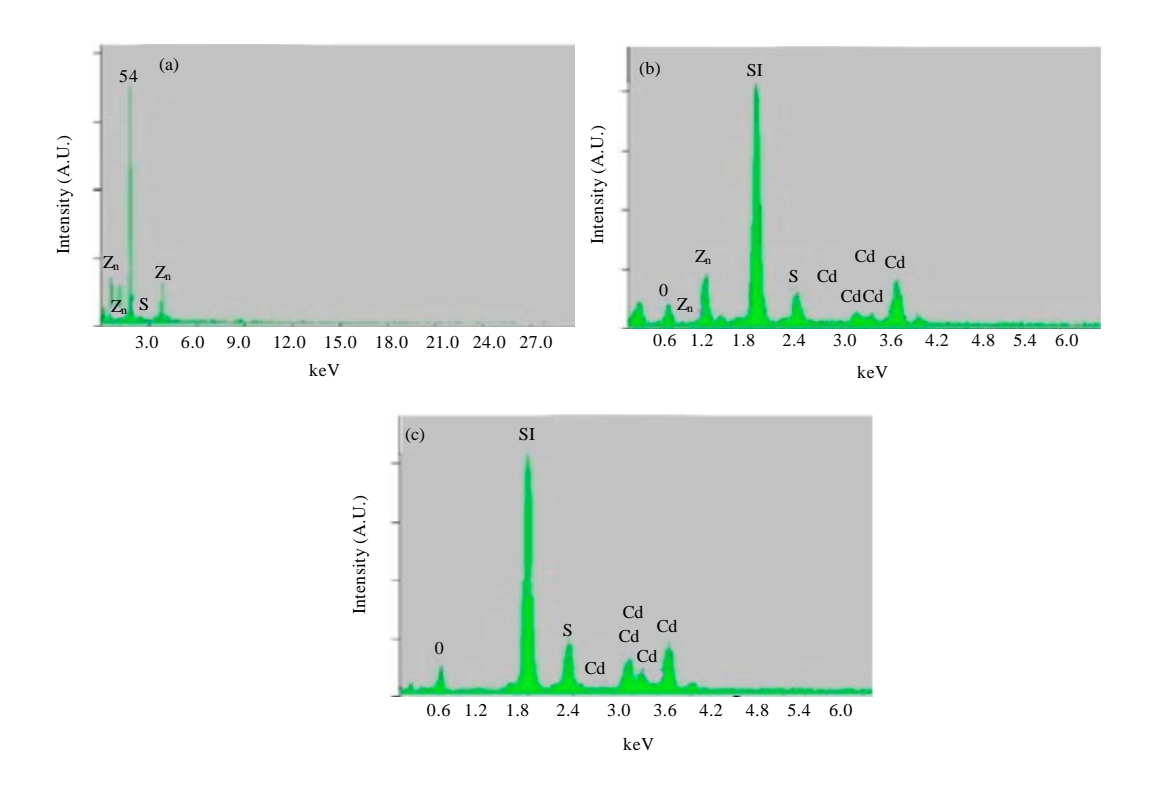


Fig. 2(a-c): EDX spectra of $Zn_{1,x}Cd_xS$ thin films for (a) x = 0.00, (b) x = 0.80 and (c) x = 1.00

X-Ray Diffraction (XRD): To check the crystallographic status of the $Zn_{1-x}Cd_xS$ films, XRD data of the as-deposited and annealed films were collected in the range 20-60 degree. The XRD patterns of as-deposited (for x = 0.80) and annealed films are shown Fig. 3. Only a broad peak is observed of the as-deposited film indicates amorphous in nature. When the film is annealed at 673 K, the amorphous nature is still remain in the film. However, annealed at 773 and 873 K, some highly resolved characteristic peaks arise on the spectra and these peaks are identified as (111, 002, 200 and 220) Millar planes for cubic, the structure according to the JCPDS chart (card no. 5-566) (Zu et al., 2009). The lattice parameter 'a' has been calculated for cubic phase using the following Eq. 1:

$$d = \frac{a}{(h^2 + k^2 + l^2)^{1/2}} \tag{1}$$

where, h, k and l are Millar indices, d is interplaner spacing and a is the lattice constant. The average value obtained is a ≈ 4.68 Å which is close to the standard value (Okoli *et al.*, 2006).

The average grain size of the film was determined for the stronger (111) and (200) peaks of each XRD patterns using Scherrer formula:

$$D_{g} = \frac{0.9\lambda}{(\Delta - 0.05^{\circ})\cos\theta}$$
 (2)

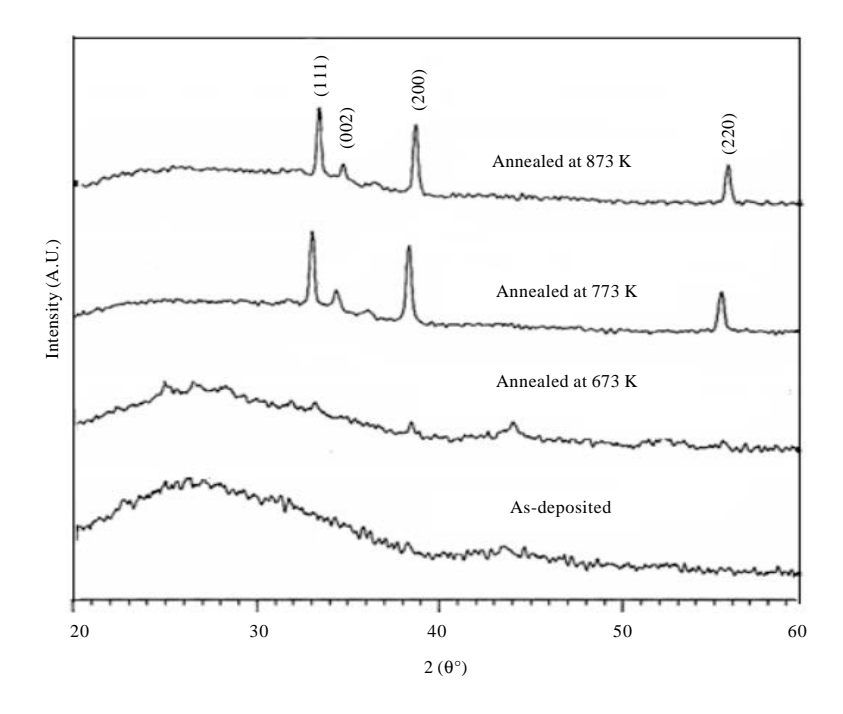


Fig. 3: X-ray diffraction patterns of Zn_{0.2}Cd_{0.8}S thin films

where, D_g is the average grain size, λ is the wavelength of the radiation used as the primary beam of $CuK_{\alpha}(\lambda=1.54178~\text{Å})$, θ is the angle of incidence in degree and Δ is the Full Width at Half Maximum (FWHM) of the peak in radian which was determined experimentally after correction of instrumental broadening (in the present case it is 0.05°). The average grain size of thin film lie in between 8 and 47 nm which indicates the nanometric size of $Zn_{0.2}Cd_{0.8}S$ grains developed in the film. The average grain size increases with the increment of annealing temperature.

Optical properties: The absorbance spectra of the as-deposited $Zn_{1x}Cd_xS$ ($0 \le x \le 1$) films are shown in Fig. 4a. Low absorption is observed in the visible and near infrared regions (540-1100 nm) and high in the ultraviolet region. Absorption increases with the increase of Cd concentration and the fundamental absorption edge shift towards the longer wavelength with cadmium contents. This nature of the absorption edge shift suggests the decrease in band gap with increasing cadmium incorporation and overall absorbance has been increased with Cd doping. This is because of the reason that in case of Cd doping, more atoms are present in the film so more states will be available for the photons to be absorbed. Figure 4b shows the optical transmittance spectra of the films. All the films demonstrate more than 65% transmittance at wavelengths longer than 540 nm which is comparable to the reported chemical bath deposition method (Ristova and Ristov, 1998) and a sharp fall in the T(%) is observed below 540 nm due to the strong absorbance of the films in this region.

The optical band gap of films is determined from the plots of $(\alpha h \mathbf{v})^2$ vs. photon energy $(h \mathbf{v})$ for direct transition (Fig. 4c). The direct band gap energy of the films were obtained from the intercept on the energy axis after extrapolation of the straight line section of $(\alpha h \mathbf{v})^2$ vs. $h \mathbf{v}$ curve to the energy axis, where $\alpha = 0$. The band gap energy of the films is varied from 3.64 (x = 0.00) to 2.40 eV (x = 1.00) of as-deposited films and 2.62-2.1 eV of annealed films shown in Table 2.

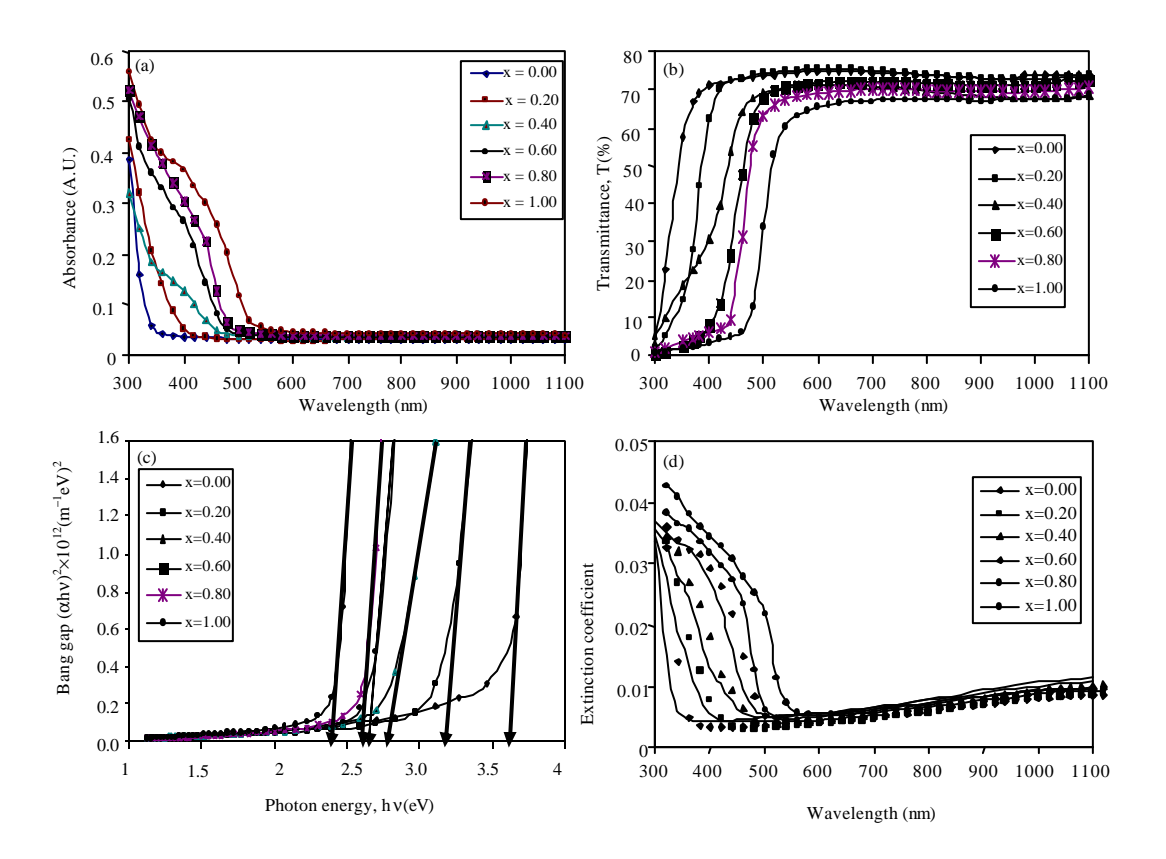


Fig. 4(a-d): (a) Absorbance, (b) Transmittance, (c) Bang gap and (d) Extinction coefficient of as-deposited Zn_{1.x}Cd_xS films

Table 2: Variation of band gap energy and Urbach energy of $\mathrm{Zn_{1-x}Cd_xS}$ thin films

Sample	Band gap (eV)	$Urbach\;energy,E_{u}\left(eV\right)$
ZnS	3.64	0.25
$\mathrm{Zn}_{0.8}\mathrm{Cd}_{0.2}\mathrm{S}$	3.16	0.29
$\mathrm{Zn}_{0.6}\mathrm{Cd}_{0.4}\mathrm{S}$	2.76	0.33
$\mathrm{Zn}_{0.4}\mathrm{Cd}_{0.6}\mathrm{S}$	2.64	0.39
$\mathrm{Zn}_{.0.2}\mathrm{Cd}_{0.8}\mathrm{S}$	2.62	0.44
CdS	2.40	0.49

The value of $E_{\rm g}$ is found to decrease from 2.62-2.10 eV with increasing annealing temperature from 673-873 K. The decrease in $E_{\rm g}$ indicates an improvement of the quality of the film due to the annealing out of the structural defects. This is in agreement with the experimental results of XRD analysis. According to XRD results, the mean grain size (for each resolved peak) increased with increased annealing temperature. As grain size increased, the grain boundary density of a film decreased, subsequently the scattering of carriers at grain boundaries decreased (Lee *et al.*, 2003). A continuous increase of optical constants and also a shift in absorption edge to a higher wavelength with increasing annealing temperature may be attributed to the improvement in the crystalline quality of the films along with reduction in porosity.

The decrease in optical bandgap energy is generally observed in the annealed direct-transition-type semiconductor films. Hong et al. (2005) observed an optical bandgap shift of

ZnO thin films from 3.31-3.26 eV after annealing and attributed this shift to the increase of the ZnO grain size. Chaparro et~al.~(2000) ascribed this 'red shift' in the energy gap, E_g to an increase in crystallite size for the annealed ZnS films. Bao et~al.~(2001) also reported a decrease in E_g with increasing annealing temperature for SrTiO₃ thin films and suggested that a shift of the energy gap was mainly due to both the quantum-size effect and the existence of an amorphous phase in thin films. In our case, the mean crystallite size increases from 8-47 nm after annealing from 673-873 K. Moreover, it is understood that the amorphous phase is reduced with increasing annealing temperature, since more energy is supplied for crystallite growth, thus resulting in an improvement in crystallinity of the $Zn_{0.2}Cd_{0.8}S$ films. Therefore, it is believed that both the increase in crystallite size and the reduction in amorphous phase amount are responsible for the bandgap decreasing in annealed $Zn_{0.2}Cd_{0.8}S$ films (Gadave et~al., 1994; Ubale and Kulkarni, 2006; Ubale et~al., 2007b).

In the case of as-deposited films, we think that this shift of the band gap with Cd incorporation resulted from the increase of carrier density or the improving donor levels and/or the possibility of structural defects in the films that give rise to the allowed states near the conduction band in the forbidden region. In case of thick films, these allowed states that could well merge with the conduction band resulting in the reduction of the band gap i.e., band gap engineering. On the other hand, when the annealing temperature is increased, the band gap was decreased as a result of the crystallinity, larger grain size growth and the decrease in defect states near the bands and these turn decrease the value of $E_{\rm g}$.

The density of localized or allowed states can be evaluated from the Urbach energy (E_u) at α <10⁴ cm⁻¹ which is referred to absorption tails at energies smaller than the optical band gap. To find the Urbach energy, a plot Ln α vs. hv was drawn and the reciprocal of the linear part gives the value of E_u . The value of Eu increases from 0.25-0.49 eV with the increment of Cd contents (Table 2) and this may be attributed to the increase of amorphousness and defects of films leading to decrease the band gap (Al-Fawade et al., 2012). The variation in the band gap energy may be useful to design a suitable tunable band gap window material in fabrication in solar cells. Our obtained E_g values are in good agreement with the published values deposited by other techniques (Raviprakash et al., 2009; Akyuz et al., 2007). The absorption coefficient (α) which is related to the other optical constants such as extinction coefficient (k), refractive index (n) and dielectric constant (α and α) were calculated from absorbance spectrum. The absorption coefficient is calculated using Beer Lambert's equation:

$$\alpha = 2.303 \left(\frac{A}{d}\right) \tag{3}$$

where, A is the optical absorbance and d is the thickness of the film. The extinction coefficient is the imaginary part of the complex index of refraction which also relates to light absorption (Xiao *et al.*, 2005). The extinction coefficient (k) is obtained from the Eq. 4:

$$k = \frac{\alpha \lambda}{4\pi} \tag{4}$$

where, λ is the wavelength.

From Fig. 4d, it is observed that the extinction coefficient increases with the increase of Cd contents. The fall in the extinction coefficient may be due to the absorption of light at the grain

Asian J. Applied Sci., 7 (7): 607-620, 2014

boundaries. The value of k decreases rapidly in the wavelength range 300-550 nm and after that it remains constant. The extinction coefficient increase rapidly when the incident photon energy exceeds band gap energy. Increase of k with the increase of hv indicates the probability of raising the electron transfers across the mobility gap with photon energy. Higher values of k represent greater attenuation or absorption of light at the grain boundaries in the thin films. The refractive index is obtained using the following Eq. 5 and 6:

$$n = \left(\frac{1+R}{1-R}\right) + \sqrt{\left(\frac{4R}{(1-R)^2} - k^2\right)}$$
 (5)

where, k is the extinction coefficient and R is the optical reflectance (Ilican *et al.*, 2007) and the reflectance has been found by using the following Eq. 6:

$$R+T+A=1 \tag{6}$$

where, T is the transmittance and A is the absorbance.

The variation of the refractive index of the films with the deposition parameter is shown in Fig. 5a. The value of n changes with Cd content are due to successive internal reflections or due to the trapped of photon within the grain boundaries. The refractive index increases sharply below the wavelength 550 nm which means it loses its energy due to various loss mechanisms such as the generation of phonons, photo generation, free carrier absorption, scattering, variety of different impurities and defects etc. It is also seen that the dispersion peak is shift towards the higher wavelength with the increase of Cd which also support to the decreased of band gap with Cd incorporation.

The variation of the real (ε_r) and imaginary (ε_i) parts of the dielectric constant for different Cd concentration are illustrated in Fig. 5b-c. The real part dielectric constant increases with Cd doping implies that slow down the speed of light in the material. The imaginary part is also increases with Cd content which gives that light absorption increases due to dipole motion or free carriers absorption. From Fig. 6d, we see that the dielectric loss increases sharply in the lower wavelength range (<550 nm) and also with Cd doping. This may be attributed to the increase of defects or amorphousness with random distribution of Cd contents.

Electrical properties: The dc electrical conductivity and sheet resistance of the as-deposited $Zn_{1-x}Cd_xS$ and annealed $Zn_{0.20}Cd_{0.8}S$ films were measured in the temperature range 303-403 K by van-der Pauw method and the experimental setup illustrated in previous study (Kamruzzaman *et al.*, 2012). The resistivity of the films was calculated using the following Eq. 7:

$$\rho = 2.265 \times t(R_{ab,cd} + R_{bc,da})$$
 (7)

where, t is the thickness of the film and $R_{ab,cd}$ and $R_{bc,da}$ are resistances for four points probe.

Variation of the conductivity with temperature of the as-deposited $\rm Zn_{1.x}Cd_xS$ and annealed $\rm Zn_{0.20}Cd_{0.8}S$ films are shown in Fig. 6a-b, respectively. From Fig. 6a, it is seen that the dc conductivity (inverse of resistivity) increases exponentially with temperature indicating that the

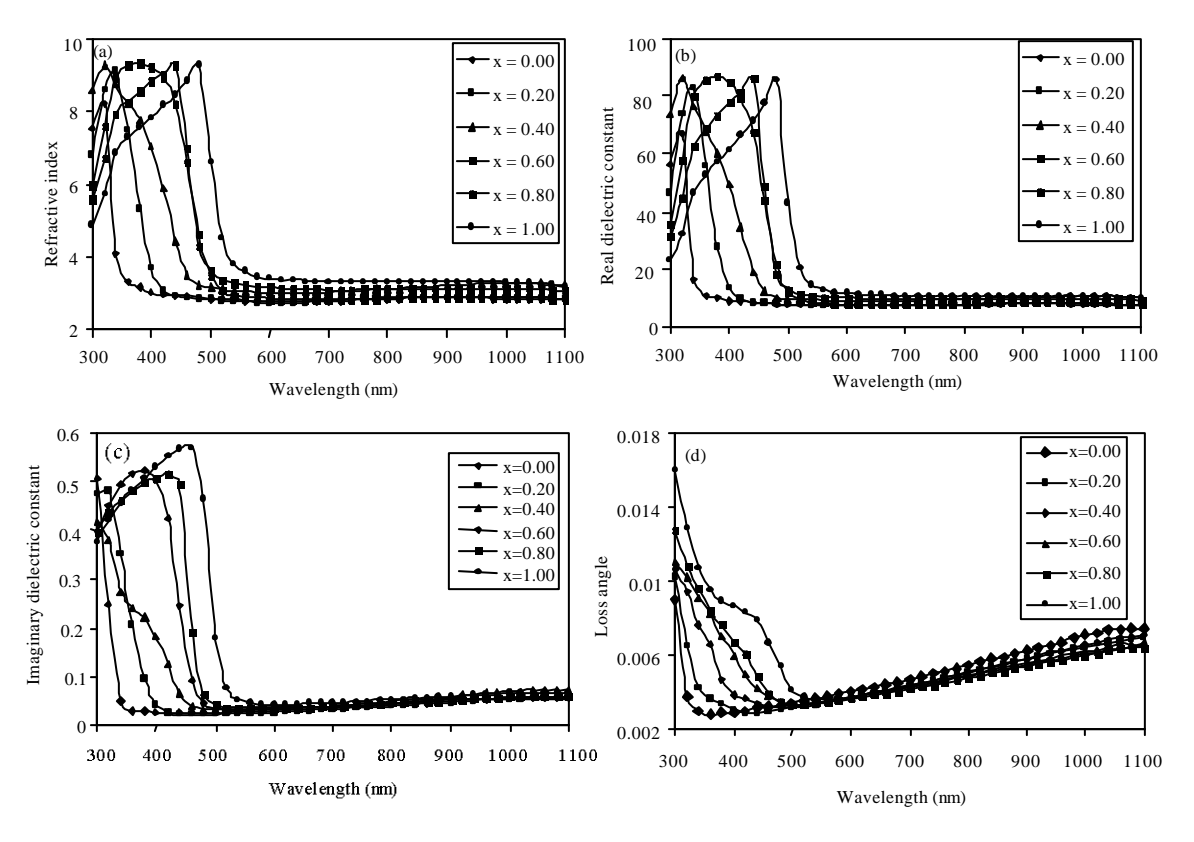


Fig. 5(a-d): (a) Refractive index, (b) Real dielectric constant, (c) Imaginary dielectric constant and (d) Loss angle of as-deposited Zn_{1-x}Cd_xS films

conductivity is a thermally activated process. Mathematically, it can be expressed by the well-known Arrhenius relation as, $\sigma_{do} = \sigma_o \exp{(-\Delta E/2 \ kT)}$.

where, σ_o is called pre-exponential factor, ΔE is called the activation energy, T is the absolute temperature and k is Boltzmann constant. The conductivity increases with the increase of temperature and also with Cd doping. This type of variation indicates the semiconducting behavior of the films. Since $Zn_{1-x}Cd_xS$ is an n-type semiconductor (Hussain $et\ al.$, 1991) and the numbers of carriers available for electrical conduction is controlled by electrons. As Cd doping increase, the number of donor levels increase and these levels slowly shift toward the conduction band of ZnS. Whenever, the temperature is increased, more and more electrons are released or hope from the donor levels and/or the valance band and goes to the conduction band. Hence, the conductivity is increased with temperature and Cd doping. Another aspect of this charge dopping mechanism is that the electron or hole tends to associate with local defects. So, the activation energy for charge transport may also include the energy of freeing the hole from its position next to the defects (Hossain $et\ al.$, 2008; Khan $et\ al.$, 2010). The annealing temperature greatly affect on the conductivity. The conductivity increases with the increase of annealing temperatures (Fig. 6b).

When the annealing temperature is increased, the surface homogeneity, quality, crystallinity increases and Cd diffuses over the surface well, reduces defects and roughness as a result of conductivity increases. The sheet resistance of the as-deposited $\rm Zn_{1x}Cd_xS$ and annealed $\rm Zn_{0.20}Cd_{0.8}S$ films follow the same mechanism as resistivity of the films (Fig. 6c-d). The activation energy of the films were determined from the $\rm ln\sigma$ vs. 1/T graph of the as-deposited $\rm Zn_{1-x}Cd_xS$ thin films and is varied from 0.021 eV (x = 0.00) to 0.1 eV (x = 1.00).

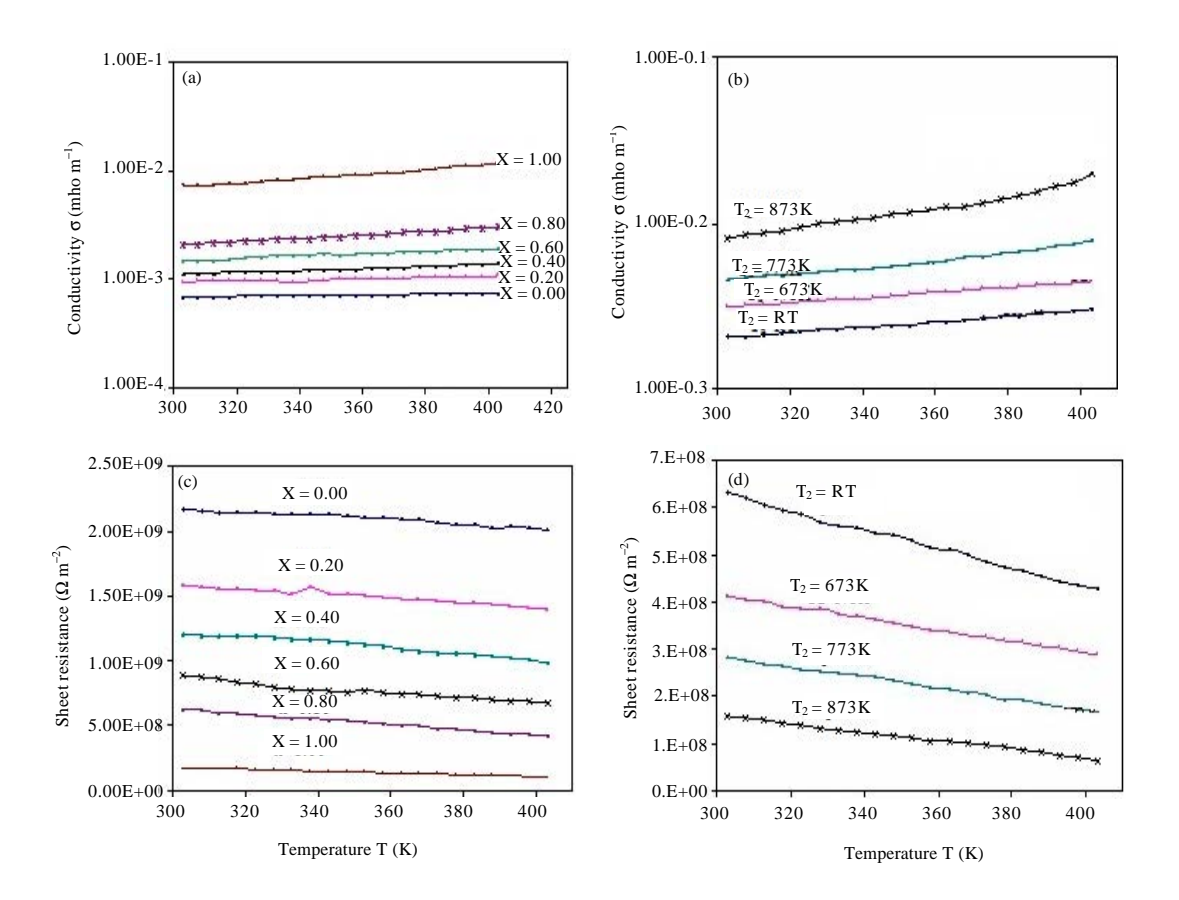


Fig. 6(a-d): Variation of (a) Electrical conductivity of as-deposited $Zn_{1-x}Cd_xS$, (b) Electrical conductivity of annealed $Zn_{0.20}Cd_{0.80}S$, (c) Sheet resistance of as-deposited $Zn_{1-x}Cd_xS$ and (d) Sheet resistance of annealed $Zn_{0.20}Cd_{0.80}S$ thin films

CONCLUSION

The prepared Zn_{1-x}Cd_xS thin films show the inhomogeneous surfaces, less defined grain boundaries. The as-deposited film contains a broad peak indicating amorphous in nature and the annealed film is found to be crystalline in nature. The average grain size of the films is found to be lying in the range of 8-47 nm and its value increases with the increase of annealing temperature. The transparency and the band gap of the films decreases with the increase of Cd doping. The direct band gap energy is varied from 3.64-2.40 eV of as-deposited Zn_{1-x}Cd_xS and 2.62-2.1 eV of the annealed films, respectively. Both as-deposited and annealed films show the semiconducting in nature in the measured temperature range. These optical and electrical results are appropriate for designing optical devices such as solar cells, optical window layers of photovoltaic cells, photodetectors, photoresistors, etc.

ACKNOWLEDGMENT

The authors would like to thank Dr. Dilip Kumar Saha Chief Scientific officer BAECD for his cordial support in performing XRD, EDX measurements. The authors are also thankful to Bangladesh University of Engineering and Technology (BUET) for financial support.

REFERENCES

- Akyuz, I., S. Kose, F. Atay and V. Bilgin, 2007. Some physical properties of chemically sprayed Zn_{1,x}Cd_xS semiconductor films. Mater. Sci. Semicond. Process., 10: 103-111.
- Al-Fawade, E.M.N., I.S. Naji and H.I. Mohammed, 2012. Study the effect of annealing temperature on the structural, optical and electrical properties of ZnS thin films. Ibn Al-Haitham J. Pure Applied Sci., 25: 150-161.
- Archbold, M.D., D.P. Halliday, K. Durose, T.P.A. Hase, D. Smyth-Boyle and K. Govender, 2005. Characterization of thin film cadmium sulfide grown using a modified chemical bath deposition process. Proceedings of the Conference Record of the 31st IEEE Photovoltaic Specialists Conference, January 3-7, 2005, Lake Buena Vista, FL., USA., pp: 476-479.
- Bao, D., X. Yao, N. Wakiya, K. Shinozaki and N. Mizutani, 2001. Band-gap energies of sol-gel-derived SrTiO₃ thin films. Applied. Phys. Lett., 79: 3767-3769.
- Bedir, M., R. Kayali and M. Oztas, 2002. Effect of the Zn concentration on the characteristic parameters of Zn_xCd_{1-x}S thin films developed by spraying pyrolysis method under the nitrogen atmosphere. Turk. J. Phys., 26: 121-126.
- Berger, L.I. and B.P. Pamplin, 1993. Properties of Semiconductors. In: Handbook of Chemistry and Physics, Lide, D.R. (Ed.). 73rd Edn., CRC Press, Boca Raton, FL., USA., pp: 12-85.
- Bhattacharjee, B., D. Ganguli, K. Iakoubovskii, A. Stesmans and S. Chaudhuri, 2002. Synthesis and characterization of sol-gel derived ZnS: Mn²⁺ nanocrystallites embedded in a silica matrix. Bull. Mater. Sci., 25: 175-180.
- Borah, J.P. and K.C. Sarma, 2008. Optical and optoelectronic properties of ZnS nanostructured thin film. Acta Physica Polonica A, 114: 713-719.
- Chaparro, A.M., M.A. Martinez, C. Guillen, R. Bayon, M.T. Gutierrez and J. Herrero, 2000. SnO₂ substrate effects on the morphology and composition of chemical bath deposited ZnSe thin films. Thin Solid Films, 361-362: 177-182.
- Chynoweth, T.A. and R.H. Bube, 1980. Electrical transport in ZnCdS films deposited by spray pyrolysis. J. Applied Phys., 51: 1844-1846.
- El Hichou, A., M. Addou, J.L. Bubendorff, J. Ebothe, B. El Idrissi and M. Troyon, 2004. Microstructure and cathodoluminescence study of sprayed Al and Sn doped ZnS thin films. Semicond. Sci. Technol., 19: 230-235.
- Gadave, K.M., S.A. Jodgudri and C.D. Lokhande, 1994. Chemical deposition of PbS from an acidic bath. Thin Solid Films, 245: 7-9.
- Glass, W., A. Kale, N. Shepherd, M. Davidson, D. DeVito and P.H. Holloway, 2007. Sputter deposited electroluminescent zinc sulfide thin films doped with rare earths. J. Vacuum Sci. Technol. A, 25: 492-499.
- Haase, M.A., J. Qiu, J.M. DePuydt and H. Cheng, 1991. Blue-green laser diodes. Applied Phys. Lett., 59: 1272-1274.
- Hall, R.B. and J.D. Meakin, 1979. The design and fabrication of high efficiency thin film CdS/Cu₂S solar cells. Thin Solid Films, 63: 203-211.
- Hirabayashi, K. and H. Kozawaguchi, 1986. ZnS: Mn electroluminescent device prepared by metal-organic chemical vapor deposition. Jpn. J. Applied Phys., 25: 711-713.
- Hong, R., J. Huang, H. He, Z. Fan and J. Shao, 2005. Influence of different post-treatments on the structure and optical properties of zinc oxide thin films. Applied Surf. Sci., 242: 346-352.
- Hussain, O.M., P.S. Reddy, B.S. Naidu, S. Uthanna and P.J. Reddy, 1991. Characterization of thin film ZnCdS/CdTe solar cells. Semicond. Sci. Technol., 6: 690-694.

- Hossain, M.S., R. Islam and K.A. Khan, 2008. Electrical conduction mechanisms of undoped and vanadium doped ZnTe thin films. Chalcogenide Lett., 5: 1-9.
- Ilican, S., M. Caglar and Y. Caglar, 2007. The effect of deposition parameters on the physical properties of Cd_xZn_{1-x}S films deposited by spray pyrolysis method. J. Optoelectron. Adv. Mater., 9: 1414-1417.
- Islam, M.R. and J. Podder, 2009. Optical properties of ZnO nano fiber thin films grown by spray pyrolysis of zinc acetate precursor. Cryst. Res. Technol., 44: 286-292.
- Jadhav, U.S., S.S. Kale and C.D. Lokhande, 2001. Effect of Cd: S ratio on the photoconducting properties of chemically deposited CdS films. Mater. Chem. Phys., 69: 125-132.
- Jayanthi, K., S. Chawla, H. Chander and D. Haranath, 2007. Structural, optical and photoluminescence properties of ZnS: Cu nanoparticle thin films as a function of dopant concentration and quantum confinement effect. Cryst. Res. Technol., 42: 976-982.
- Kamruzzaman, M., T.R. Luna, J. Podder and M.G.M. Anowar, 2012. Synthesis and characterization of Cd_{1-x}Co_xS thin films prepared using the spray pyrolysis technique. Semicond. Sci. Technol., Vol. 27. 10.1088/0268-1242/27/3/035017
- Kanemitsu, Y., T. Nagai, T. Kushida, S. Nakamura, Y. Yamada and T. Taguchi, 2002. Free excitons in cubic CdS films. Applied Phys. Lett., 80: 267-269.
- Khan, M.K.R., M.A. Rahman, M. Shahjahan, M.M. Rahman, M.A. Hakim, D.K. Saha and J.U. Khan, 2010. Effect of Al-doping on optical and electrical properties of spray pyrolytic nano-crystalline CdO thin films. Curr. Applied Phys., 10: 790-796.
- Kulkarni, S.K., U. Winkler, N. Deshmukh, P.H. Borse, R. Fink and E. Umbach, 2001. Investigations on chemically capped CdS, ZnS and ZnCdS nanoparticles. Applied Surf. Sci., 169: 438-446.
- Kumar, V., M.K. Sharma, J. Gaur and T.P. Sharma, 2008. Polycrystalline ZnS thin films by screen printing method and its characterization. Chalcogenide Lett., 5: 289-295.
- Lee, J.H., K.H. Ko and B.O. Park, 2003. Electrical and optical properties of ZnO transparent conducting films by the sol-gel method. J. Cryst. Growth, 247: 119-125.
- Lytvyn, O.S., V.S. Khomchenko, T.G. Kryshtab, P.M. Lytvyn and M.O. Mazin *et al.*, 2001. Structural investigations of annealed ZnS: Cu, Ga film phosphors. Semicond. Phys. Quantum Electron. Optoelectron., 4: 19-23.
- Marquardt, E., B. Opitz, M. Scholl and M. Heuken, 1994. Electroabsorption and light modulation with ZnSe/ZnSSe multiquantum wells grown by metalorganic vapor phase epitaxy. J. Applied Phys., 75: 8022-8026.
- Nakada, T., N. Okano, Y. Tanaka, H. Fukuda and A. Kunioka, 1994. Superstrate-type CuInSe₂ solar cells with chemically deposited CdS window layers. Proceedings of the IEEE 1st World Conference on Photovoltaic Energy Conversion, Volume 1, December 5-9, 1994, Waikoloa, HI., USA., pp: 95-98.
- Nicolau, Y., M. Dupuy and M. Bruuel, 1990. ZnS, CDS and Zn_{1.x}Cd_xS thin films deposited by the successive ionic layer adsorption and reaction process. J. Electrochem. Soc., 137: 2915-2924.
- Okoli, D.N., A.J. Ekpunobi and C.E. Okeke, 2006. Growth and characterization of ZnCdS thin films by chemical bath deposition technique. Acad. Open Internet J., 18: 1-12.
- Oladeji, I.O., L. Chow, C.S. Ferekides, V. Viswanathan and Z. Zhao, 2000. Metal/CdTe/CdS/Cd_{1-x}Zn_xS/TCO/glass: A new CdTe thin film solar cell structure. Solar Energy Mater. Solar Cells, 61: 203-211.

Asian J. Applied Sci., 7 (7): 607-620, 2014

- Oztas, M. and M. Bedir, 2001. Low resisitivity of the chemically deposited CdS and ZnCdS thin films for use as windows in heterojunction solar cells. Pak. J. Applied Phys., 1: 214-217.
- Raviprakash, Y., K.V. Bangera and G.K. Shivakumar, 2009. Preparation and characterization of $\mathrm{Cd_{x}Zn_{1-x}S}$ thin films by spray pyrolysis technique for photovoltaic applications. Solar Energy, 83: 1645-1651.
- Reddy, K.R. and P.J. Reddy, 1992. Studies of $Zn_xCd_{1-x}S$ films and $Zn_xCd_{1-x}S/CuGaSe_2$ heterojunction solar cells. J. Phys. D: Applied Phys., 25: 1345-1348.
- Ristova, M. and M. Ristov, 1998. Silver-doped CdS films for PV application. Solar Energy Mater. Solar Cells, 53: 95-102.
- Saraf, R., 2012. High efficiency and cost effective Cu₂S/CdS thin-film solar cell. J. Electr. Electron. Eng., 2: 47-51.
- Seo, K.W., W. Kook, S.H. Yoon, S.S. Lee and W. Shim, 2005. Preparation of ZnS thin film using Zn(dithiocarbamate)₂ precursors by MOCVD method. Bull. Korean Chem. Soc., 26: 1582-1584.
- Shaban, S.M., N.M. Saeed and R. AL-Haddad, 2011. Fabrication and study zinc sulfide schottky barrier detectors. Indian J. Sci. Technol., 4: 384-386.
- Torres, J. and G. Gordillo, 1992. Photoconductors based on Zn_xCd_{1-x}S thin films. Thin Solid Films, 207: 231-235.
- Ubale, A.U. and D.K. Kulkarni, 2006. Studies on size dependent properties of cadmium telluride thin films deposited by using successive ionic layer adsorption and reaction method. Indian J. Pure. Applied Phys., 44: 254-259.
- Ubale, A.U., V.S. Sangawar and D.K. Kulkarni, 2007a. Size dependent optical characteristics of chemically deposited nanostructured ZnS thin films. Bull. Mater. Sci., 30: 147-151.
- Ubale, A.U., A.R. Junghare, N.A. Wadibhasme, A.S. Daryapurkar, S.B. Mankar and V.S. Sangawar, 2007b. Thickness dependent structural, electrical and optical properties of chemically deposited nanopartical PbS thin films. Turk. J. Phys., 31: 279-286.
- Xiao, H., Z. Xianogyan, A. Uddin and C.B. Leu, 2005. Preparation and characterization of electronic and optical properties of plasma polymerized nitrites. Thin Solid Films, 477: 81-87.
- Yamaguchi, T., J. Matsufusa and A. Yoshida, 1992. Optical transitions in RF sputtered $CuIn_xGa_1$ _xSe₂ thin films. Jpn. J. Appl. Phys., 31: L703-L705.
- Zu, S., Z. Wang, B. Liu, X. Fan and G. Qian, 2009. Synthesis of nano-Cd_x Zn_{1-x} S by precipitate-hydrothermal method and its photocatalytic activities. J. Alloys Compounds, 476: 689-692.